HAL
open science

Structural and magnetic properties of the (Ca1-xNax)(Fe2-xTix)O4 solid solution (0 x 1)

Siwar Zouari, Laurent Ranno, Abdelwaheb Cheikh-Rouhou, Olivier Isnard, Pierre Wolfers, Pierre Bordet, Pierre Strobel

To cite this version:

Siwar Zouari, Laurent Ranno, Abdelwaheb Cheikh-Rouhou, Olivier Isnard, Pierre Wolfers, et al.. Structural and magnetic properties of the (Ca1-xNax)(Fe2-xTix)O4 solid solution (0 x 1). Journal of Alloys and Compounds, 2008, 452 (2), pp.234-240. 10.1016/j.jallcom.2007.01.074 . hal-00186056

HAL Id: hal-00186056

https://hal.science/hal-00186056

Submitted on 9 Nov 2007

HAL is a multi-disciplinary open access archive for the deposit and dissemination of scientific research documents, whether they are published or not. The documents may come from teaching and research institutions in France or abroad, or from public or private research centers.

L'archive ouverte pluridisciplinaire **HAL**, est destinée au dépôt et à la diffusion de documents scientifiques de niveau recherche, publiés ou non, émanant des établissements d'enseignement et de recherche français ou étrangers, des laboratoires publics ou privés.

Structural and magnetic properties of the $(Ca_{1-x}Na_x)(Fe_{2-x}Ti_x)O_4$ solid solution ($0 \leq x \leq 1$)

S. Zouari[a,b], L. Ranno[b], A. Cheikh-Rouhou[a], O. Isnard[b], P. Wolfers[b], P. Bordet[b] and P. Strobel[b†]

[a]*Laboratoire de Physique des Matériaux, Faculté des Sciences de Sfax, B. P. 763, 3038 Sfax, Tunisie.*

[b]*Institut Néel, CNRS, B. P. 166, 38042 Grenoble, Cedex 9 France.*

Abstract

New compounds corresponding to the $(Ca_{1-x}Na_x)(Fe_{2-x}Ti_x)O_4$ formula with $0 \leq x \leq 1$ were prepared by solid state reactions at 1100 °C in air. A continuous solid solution was found between end members $CaFe_2O_4$ and $NaFeTiO_4$. The evolution of structural parameters and bonding geometry with composition is discussed in detail. Magnetic measurements show that the antiferromagnetic ordering known in $CaFe_2O_4$ is suppressed for all x values investigated ($x \geq 0.2$). The absence of crystallographic transition at low temperature was checked by X-ray diffraction down to 10 K. The magnetic structure of $CaFe_2O_4$ was redetermined from powder neutron diffraction. Spins on the two iron sites order antiparallel (F_zF_z spin arrangement), as described previously. The difference in magnetic moments on Fe1 and Fe2 sites result in a ferrimagnetic configuration with net moment 2.72 μ_B at 2 K.

Keywords: oxide materials; crystal structure; magnetic measurements; neutron diffraction

Corresponding author
Postal address: Institut Néel-Cristallographie, CNRS, BP 166, 38042 Grenoble Cedex 9, France
e-mail: pierre.strobel@grenoble.cnrs.fr

Introduction

Calcium ferrite, $CaFe_2O_4$, cristallizes in an orthorhombic structure, space group Pnma, containing two iron octahedral sites Fe1 and Fe2. The structure is made up of distorted FeO_6 octahedra sharing edges and corners, and eight-fold coordinated calcium atoms [1, 2]. This structure type (or distorted variants of it) is encountered not only in various CaM_2O_4 phases (M = Ti, V, Mn), but also in sodium compounds with charge distribution $NaM^{3+}M'^{4+}O_4$; examples are known with B = Sc, Fe and B' = Ti, Sn [3]. The crystal structures of all these phases belong to the same space group (Pbnm) as $CaFe_2O_4$.

$CaFe_2O_4$ is known to exhibit a ferrimagnetic structure below T_c = 160 K [4, 5]. The spin arrangement was determined in the 60s [4, 5]. It is characterized by an antiparallel alignment of Fe1 and Fe2 spins along the b axis in Pnma setting [5] (the older literature often used a Pbnm cell with a different axis setting). In view of this interesting magnetic structure, and of the structural similarity between the calcium and sodium phases, we undertook a study of the solid solution $(1\text{-}x)CaFe_2O_4$, $xNaFeTiO_4$, or $(Ca_{1-x}Na_x)(Fe_{2-x}Ti_x)O_4$.

In this paper, we report the synthesis, structural and magnetic study of this solid solution, which is found to exist in the whole concentration range ($0 \leq x \leq 1$). Magnetic measurements will show that $CaFe_2O_4$ is the only compoud in the series showing magnetic ordering : this feature is suppressed for titanium substitution levels as low as 10 % (x = 0.2). The crystal and magnetic structure of $CaFe_2O_4$ was redetermined from X-ray and neutron diffraction data at low temperature.

Experimental

Powder samples of $CaFe_2O_4$ and $NaFeTiO_4$ were synthesized by a conventional solid-state ceramic method starting from stoichiometric mixtures of $CaCO_3$, $NaCO_3$, TiO_2 and Fe_2O_3 (>99.9% purity). The starting materials are mixed in an agate mortar and fired in air repeatedly at 1200°C in air with intermediate regrindings.

Members of the $(Ca_{1-x}Na_x)(Fe_{2-x}Ti_x)O_4$ solid solution were obtained using the end members $CaFe_2O_4$ and $NaFeTiO_4$ as precursors. Mixtures in appropriate proportions were pressed into pellets and fired in air, initially at 1000°C, then twice at 1100 °C for 48 h, with intermediate regrinding and furnace cooling.

Phase purity, homogeneity, and unit cell dimensions were determined by powder X-ray diffraction with a Bruker D8 diffractometer equipped with a Kevex Si(Li) solid detector and CuK_{α} radiation and operating in transmission geometry. Intensities were recorded from 11 to 91° 2θ with a 0.025 2θ step and 80 s counting time per step. A rotating sample holder was used to minimize preferential orientation effects.

Magnetization measurements were performed using an extraction magnetometer in the temperature range 10-300 K. Studies of magnetization as a function of applied field were carried out up to 8T.

In order to determine the magnetic structure, neutron diffraction experiments were carried out at Institut Laue-Langevin (Grenoble, France) , using the high flux D1B diffractometer (position sensitive detector of 400 cells). Patterns were collected at 0.02° intervals of 2θ from 24.00 to 88.00° using a wavelength of 2.52 Å at 2K steps in the temperature range 1.5-300 K. An additional diffractogram was recorded with 1.28504 Å at 280 K in order to collect a larger number of reflections for structure refinement.

Because of the small number of reflections available in the neutron diffraction study, an additional X-ray powder thermodiffraction study was carried out, in order to check for possible distortion at low temperature. This was achieved in the temperature range 3–470K using a bath cryostat with kapton windows mounted on a high-resolution diffractometer operating in Bragg-Brentano focusing geometry (primary beam focusing quartz monochromator , Cr $K_{\alpha 1}$ radiation) [6].

The nuclear and magnetic structures were analyzed with the Rietveld method using the Fullprof [7] and MXD [8] software programs, respectively.

Results and discussion

Solid solution and crystallographic structure

Fig 1 shows the evolution of the X-ray patterns as a function of Ti content x. All patterns are indexable in space group Pnma; no impurity lines were detected. The cell parameters are given in Table 1 (upper part). The simultaneous substitution of iron by titanium and of calcium by sodium leads to a monotonous decrease of a and b cell parameters (see Figure 2). On the contrary, c initially increases up to a maximum value for $x \approx 0.8$, then decreases slightly on the titanium-rich side (see Figure 2c). The overall evolution corresponds to a small (1.9 %) cell volume decrease (see Figure 2d). It should be

noted that this double substitution corresponds to rather small ion size changes between the pairs Fe^{3+} (0.64 Å) – Ca^{2+} (1.00 Å) and Ti^{4+} (0.605 Å) – Na^{+} (1.02 Å), according to Shannon's octahedral radii scale [9].

The crystal structures of all solid solution members were refined using the Rietveld method. Each atom lies in position 4c: x, 1/4, z in the Pnma space group. Table 1 summarizes the refinement results and includes final atomic and thermal parameters, and statistical parameters (the well-known compound $CaFe_2O_4$ was run on a Siemens D5000 diffractometer with poorer resolution, explaining the differences in refinement statistics). Figure 3 shows typical refinement results. Regarding the occupation of iron and titanium on the two transition metal sites M1 and M2, no significant preference of titanium for either site was found. This is consistent with the situation in the $NaFeTiO_4$ end member, where previous studies concluded to a statistical distribution of iron and titanium [10].

$CaFe_2O_4$ and $NaFeTiO_4$ are expected to be stoichiometric [1-3]; this is confirmed by their colour, which is light brown for both compounds, in agreement with a strictly Fe^{3+} oxidation state. High-temperature treatments, however, might introduce oxygen or sodium vacancies. This possibility was checked by refinements including variable occupations for sodium and the four oxygen positions ; in all cases, the refined occupation factors were not significantly different from 1.

The evolution of distances and angles is given in Table 2. With increasing Na-Ti content, both Fe-O1 and Fe-O2 show a parallel evolution with a very slight bond length increase, followed by a decrease, as expected from the smaller Ti^{4+} ionic radius (see Figure 4). In fact, consideration of average bond lengths is not very satisfying in this case, because of the rather irregular distribution of distances and angles around the Fe/Ti site (see Table 2). The evolution of the structure with composition may be better understood considering the Fe1-O-Fe2 octahedra pairs which form the basic structural unit. As shown in Figure 5, the Fe1 bond to the linking oxygen O1 decreases significantly with increasing x (from 2.03 to 1.90 Å), whereas the length of the other "arm" of this bridge, i.e. the Fe2-O1 bond, simultaneously increases (from 2.039 to 2.088 Å). The bond angles also exhibit significant changes : values for the two bridging oxygen atoms O1 and O3 are indicated in Figure 5, showing "breathing" of the bonds connecting the Fe1 and Fe2 edge-sharing octahedra with composition change. The Fe1-O3-Fe2 angle, in particular, shows a maximum for x = 0.5-0.6, possibly connected with the odd variation of the c parameter.

Magnetic behaviour

The temperature dependence of the magnetization for various compositions is given in Figure 6. The magnetization decreases with increasing Na-Ti content, in agreement with the dilution of the magnetic species Fe^{3+}. As expected for an ferrimagnetic material, the $CaFe_2O_4$ curve exhibits a wide anomaly below $T_C \approx 160$ K. Such a behaviour is clearly absent in all other samples, meaning that substitution of as little as 10 % Fe by Ti (as for x = 0.2) completely suppresses antiferromagnetic ordering. So it seems that the long-range antiferromagnetic ordering between Fe1 and Fe2 spins is so sensitive to local magnetic exchange perturbations that it cannot take place when 10 % Fe1 and Fe2 atoms are randomly substituted by a diamagnetic species.

Magnetic structure of $CaFe_2O_4$

Magnetic measurements showed the disappearance of antiferromagnetic ordering in all substituted $CaFe_2O_4$ samples. Consequently only unsubstituted $CaFe_2O_4$ was submitted to an X-ray and neutron thermodiffraction study. Low-temperature X-ray measurements showed that the crystal structure is unchanged on cooling down to 10 K.

The evolution of the neutron powder diffraction (NPD) pattern below $T_N = 160$ K is shown in Figure 8. It shows the emergence of extra reflections below T_N, as well as intensity increases of other permitted reflections, indicating the onset of a magnetic ordering. All magnetic peaks can be indexed in the crystallographic unit cell, showing that the propagation vector *k* is equal to [000].

In order to solve the magnetic structure, the irreducible representations and the basis functions of each representation were calculated by applying the projection operator technique [11-13] (see Table 3). The following modes were used for the two iron atom sites :

$F = S_1 + S_2 + S_3 + S_4$

$G = S_1 - S_2 + S_3 - S_4$

$C = S_1 + S_2 - S_3 - S_4$

$A = S_1 - S_2 - S_3 + S_4$

All possible combinations of spins in the magnetic cell were tested against neutron powder diffraction data. The collinear representation Γ_4 gives the best agreement with the observed intensities and confirms that the magnetic moments are ordered in a (F_zF_z) spin

arrangement. The results of X-ray and neutron refinements at low temperature are summarized in Table 4.

The z-component of the magnetic moments M_z are found to be 4.49 μ_B for Fe_1 and -1.77 μ_B for Fe_2, resulting in a net magnetic moment of 2.72 μ_B, to be compared with 2.22 μ_B obtained in the older study by Bertaut et al.[5].

Conclusions

We showed in this work that $CaFe_2O_4$ and $NaFeTiO_4$ form a continuous range of solid solution with simultaneous substitution of sodium for calcium and of titanium for half of iron. Titanium is distributed randomly on the two iron sites, within the accuracy of structural refinements. This double substitution results in subtle variations in bond lengths and angle, with an slight overall cell volume decrease with increasing Na-Ti content. The introduction of 10 % titanium on iron sites is sufficient to prevent the onset of magnetic ordering. Finally, the crystal and magnetic structure of $CaFe_2O_4$ was checked using both X-ray and neutron diffraction at low temperature. The crystal structure is unchanged, and the ferrimagnetic structure proposed earlier by Bertaut et al. is confirmed.

References

[1] O. Muller and R. Roy, *The Major Ternary Structural Families* , Springer, Berlin, 1974, p.55.

[2] T. Irifune, K. Fujino and E. Ohtani, *Nature* **349** (1991) 409-411.

[3] A. F. Reid, A. D. Wadsley, M. J. Sienko, *Inorg. Chem.* **7** (1968) 112-115.

[4] Y. Allain and B. Boucher, *J. de Phys. (Paris)* **26** (1965) 789-792.

[5] E.F Bertaut, J. Chappert, A. Apostolov and V. Semenov, *Bull. Soc. Franç. Minéral. Cristallogr*. **89** (1966) 206-212.

[6] P. Fertey and F. Sayetat, *J. Appl. Cryst.* **29** (1996) 692-699.

[7] J. Rodriguez-Carvajal, *Physica B.* **55** (1993) 192-193.

[8] P. Wolfers, J. Appl. Crystallogr. **23** (1990) 554-557.

[9] R. D. Shannon, *Acta. Crystallogr.* **A32** (1976) 751-754.

[10] W.G. Mumme and A.F. Reid, *Acta. Crystallogr.* **B24** (1968) 625-631.

[11] E. F. Bertaut, *Acta. Crystallogr.* **A24** (1968) 217-222.

[12] C. J. Bradley and A. P. Cracknell, *The Mathematical Theory of Symmetry in Solids*, Clarendon Press, Oxford, 1972.

[13] S. Zouari, L. Ranno, A. Cheikh-Rouhou, O. Isnard, M. Pernet, P. Wolfers, P. Strobel *J. Alloys and Compounds* **353** (2003) 5.

Figure Captions

Fig. 1. XRD patterns of $(Ca_{1-x}Na_x)(Fe_{2-x}Ti_x)O_4$ compounds with various values of x.

Fig. 2. Evolution of cell parameters a, b, c and of cell volume (d) throughout the $(Ca_{1-x}Na_x)(Fe_{2-x}Ti_x)O_4$ as a function of x. The lines are a guide to the eye.

Fig. 3. Observed (points) and calculated (continuous line) X-ray powder diffraction patterns for x = 0.2 and x = 0.8. The lower part shows the difference I_{obs}–I_{calc}.

Fig. 4. Evolution of Fe(Ti)-O distances across the $(Ca_{1-x}Na_x)(Fe_{2-x}Ti_x)O_4$ solid solution. The lines are a guide to the eye.

Fig. 5. Comparison of the iron and bridging oxygen environments for three compositions x = 0, 0.5 and 1.

Fig. 6. Variation of magnetization of various $(Ca_{1-x}Na_x)(Fe_{2-x}Ti_x)O_4$ compositions as a function of temperature. Data measured in a 0.2 T applied field

Fig. 7. Thermal evolution of the $CaFe_2O_4$ neutron diffraction pattern (measured at λ = 2.289 Å).

Figure1

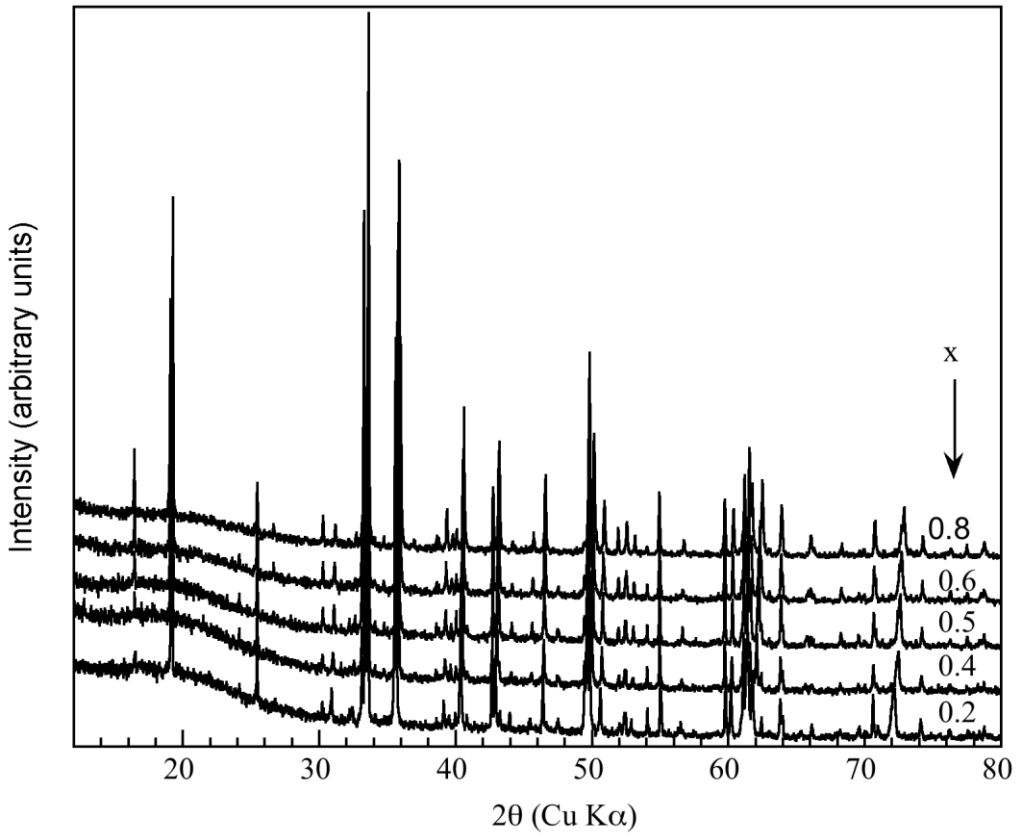
Intensity (arbitrary units)
x
0.8
0.6
0.5
0.4
0.2
20
30
40
50
60
70
80
2θ (Cu Kα)

Figure 2

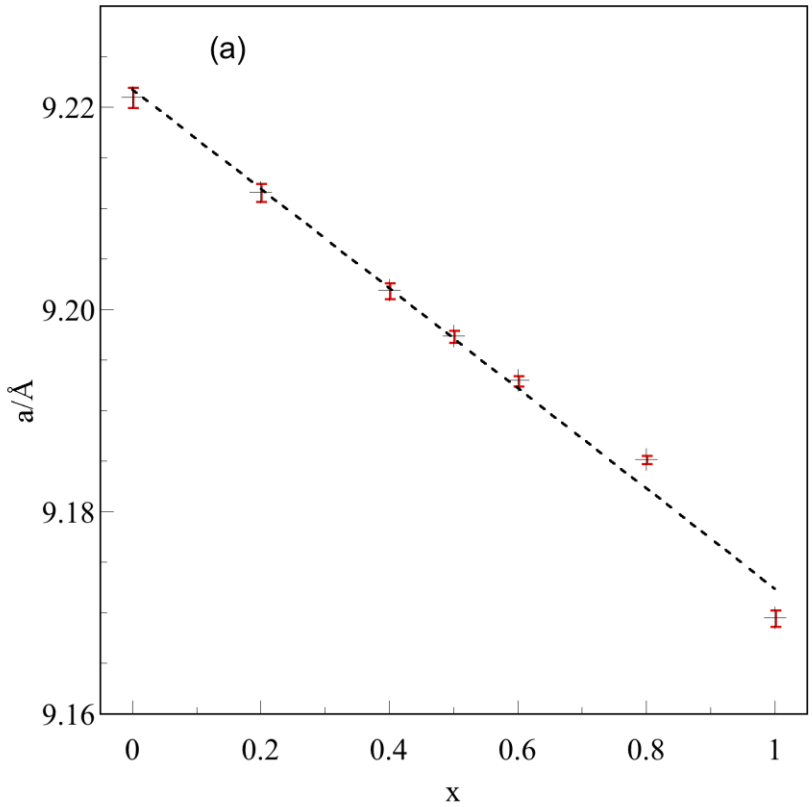
(a)
9.22
9.20
9.18
9.16
a/Å
0
0.2
0.4
0.6
0.8
1
x

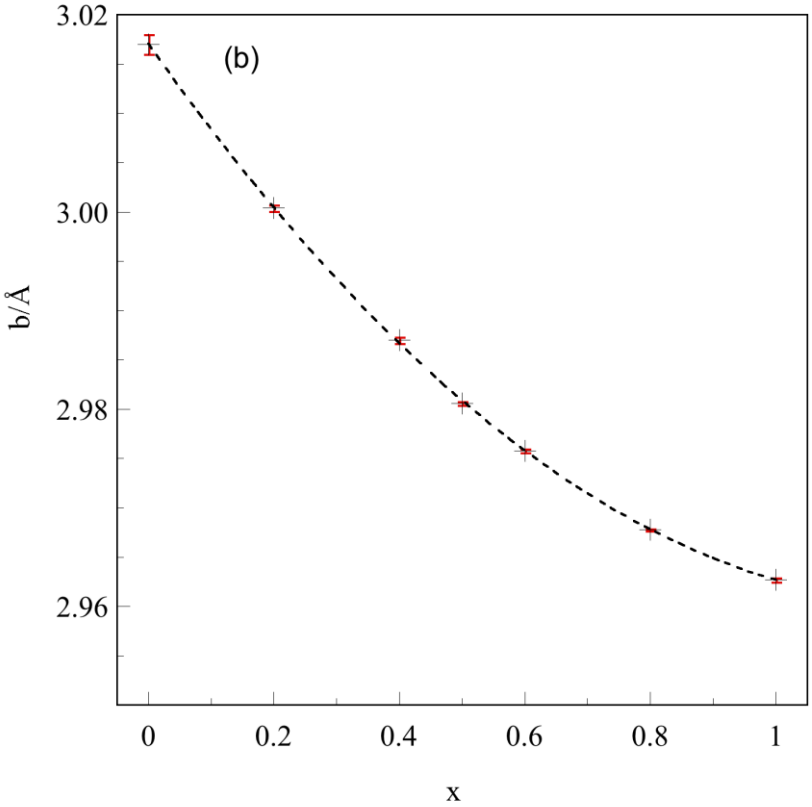
(b)
3.02
3.00
2.98
2.96
b/Å
0
0.2
0.4
0.6
0.8
1
x

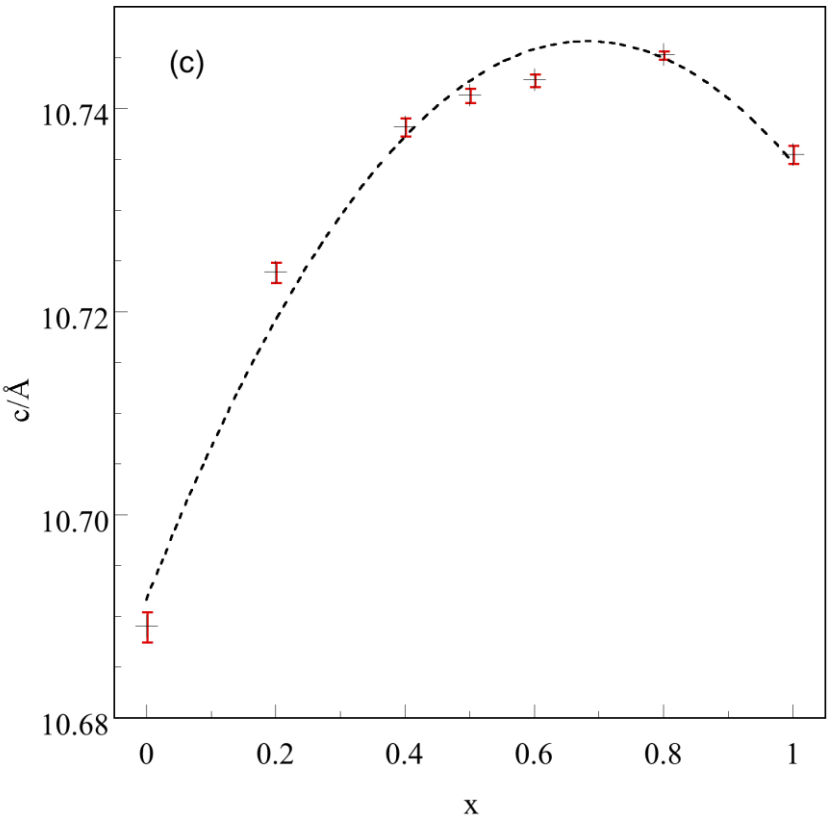
(c)
10.74
10.72
10.70
10.68
c/Å
0
0.2
0.4
0.6
0.8
1
x

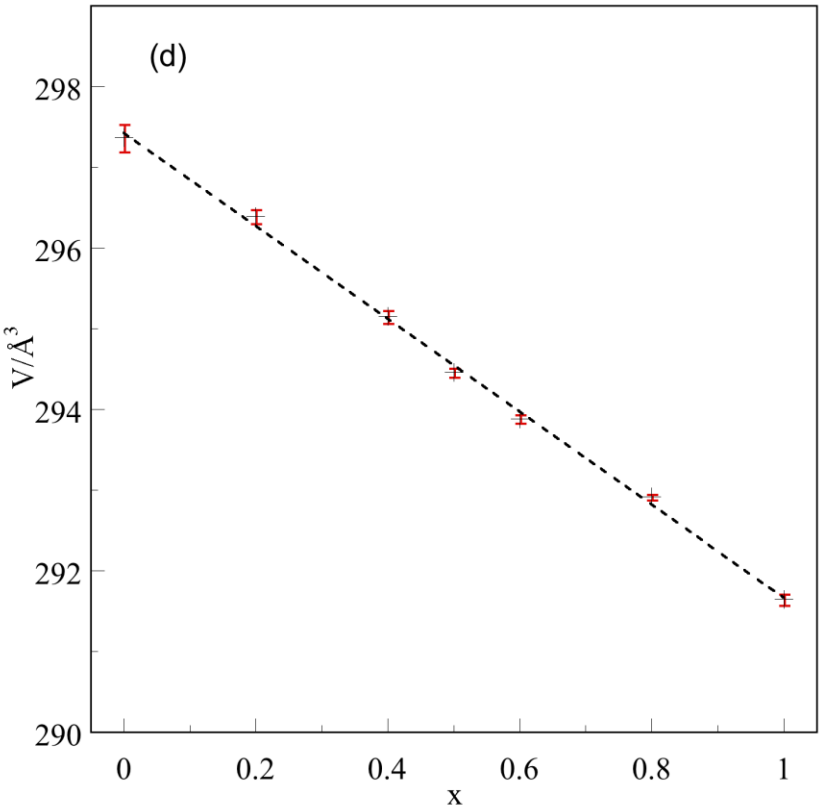
(d)
298
296
294
292
290
V/Å^3
0
0.2
0.4
0.6
0.8
1
x

Figure 3

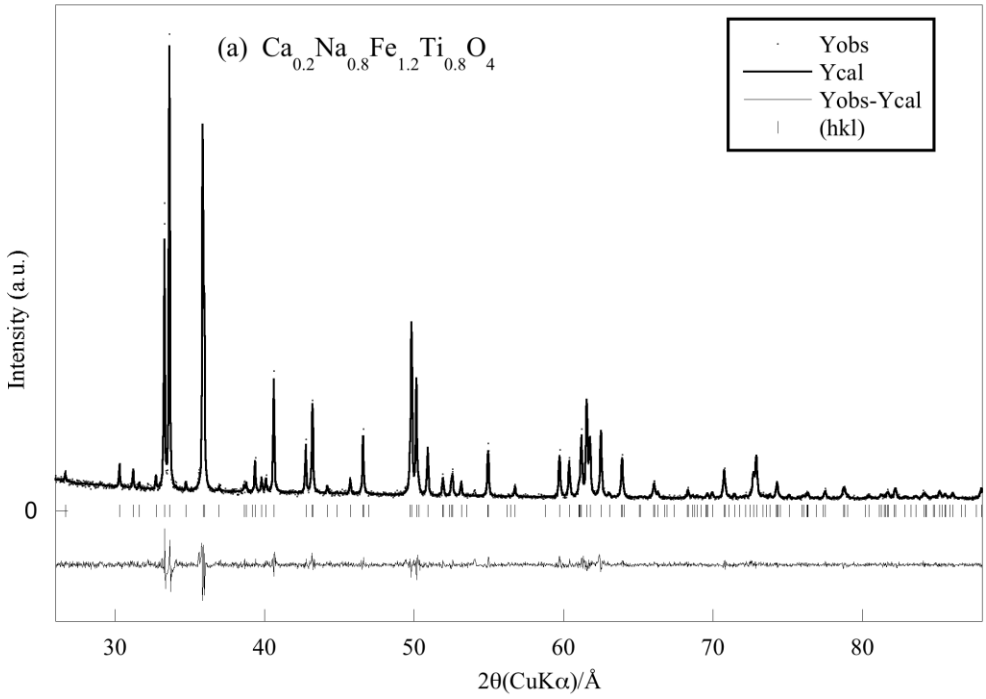
(a) $Ca_{0.2}Na_{0.8}Fe_{1.2}Ti_{0.8}O_4$
Yobs
Ycal
Yobs-Ycal
(hkl)
Intensity (a.u.)
0
30
40
50
60
70
80
2θ(CuKα)/Å

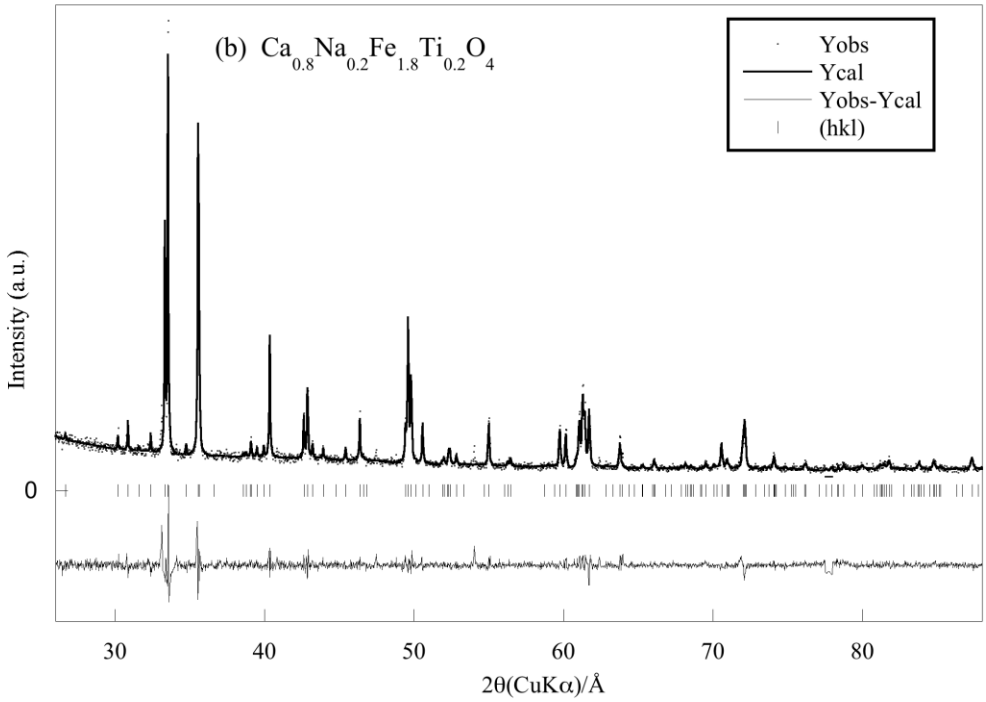
(b) $Ca_{0.8}Na_{0.2}Fe_{1.8}Ti_{0.2}O_4$
Yobs
Ycal
Yobs-Ycal
(hkl)
Intensity (a.u.)
0
30
40
50
60
70
80
2θ(CuKα)/Å

Figure 4

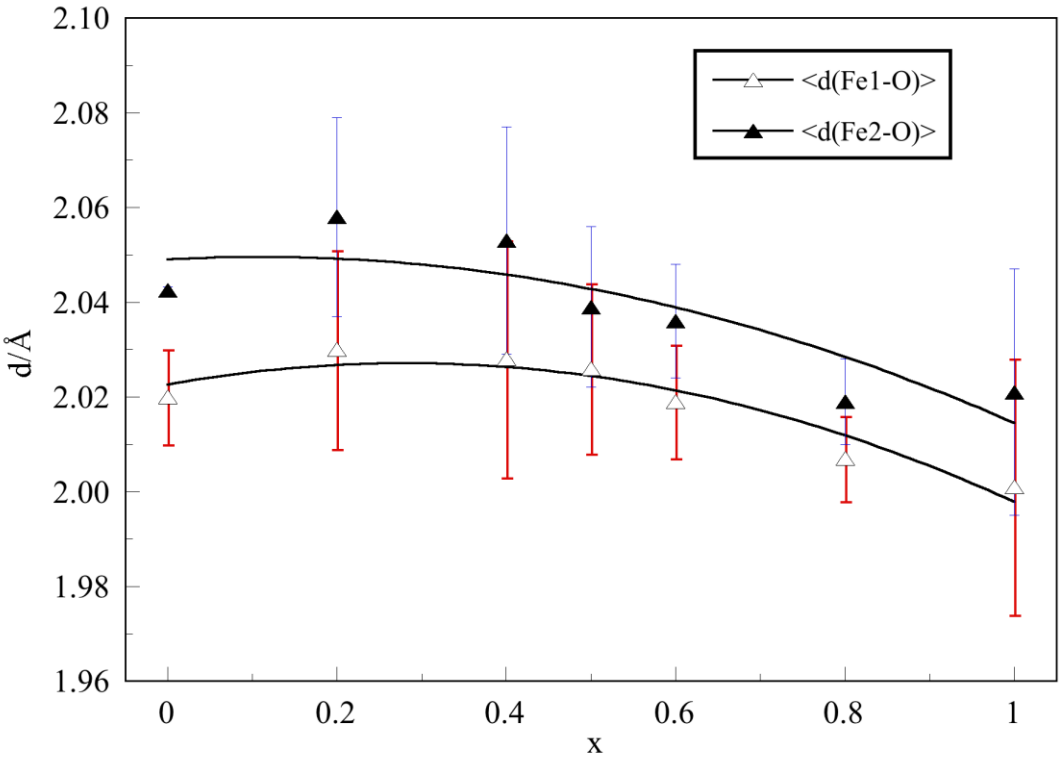

Figure 5

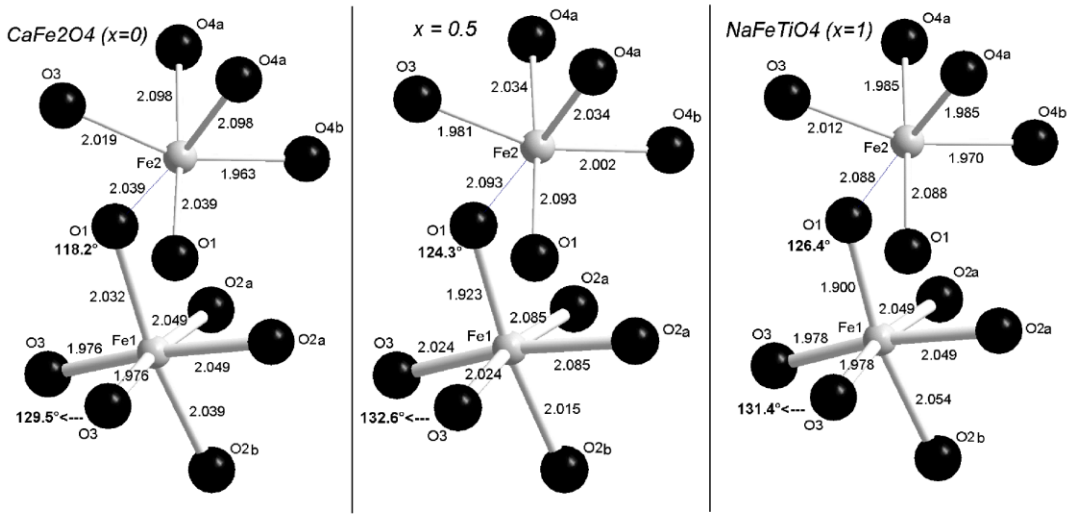

Figure 6

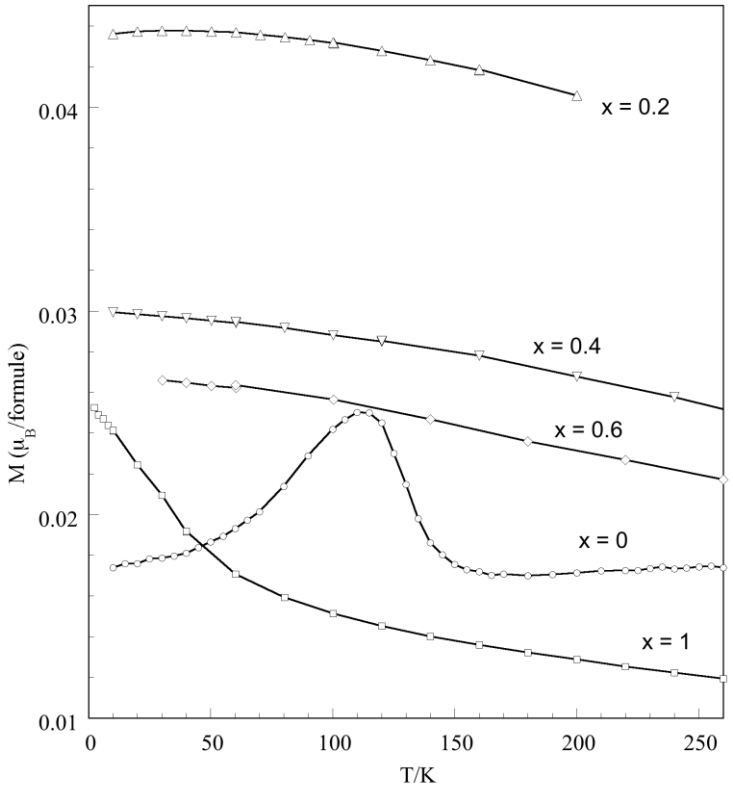

Figure 7

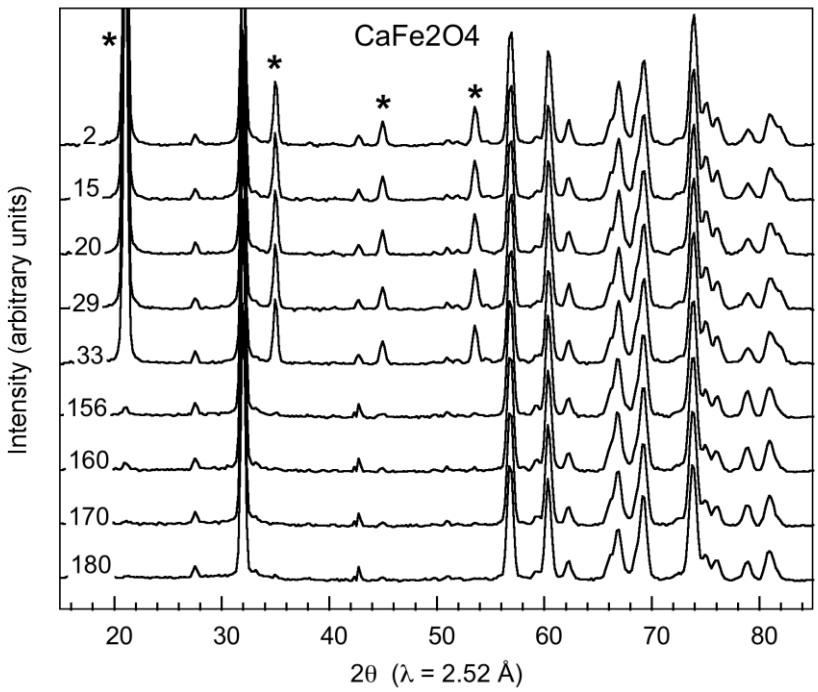

Table 1. Results of Rietveld refinements along the $CaFe_2O_4$-$NaFeTiO_4$ solid solution (from XRD data at room temperature). Space group Pnma

	x	**0**	**0.2**	**0.4**	**0.5**	**0.6**	**0.8**	**1**
cell parameters (Å)								
	a	9.922(1)	9.2116(9)	9.2019(8)	9.1974(6)	9.1930(5)	9.1852(4)	9.1695(8)
	b	3.017(1)	3.0004(3)	2.9870(3)	2.9806(2)	2.9758(2)	2.9678(2)	2.9627(2)
	c	10.689(2)	10.724(1)	10.7382(9)	10.7413(7)	10.7428(6)	10.7453(4)	10.7355(9)
Positional and thermal parameters (all atoms in 4c position, y = ¼)								
Ca(Na)	*x*	0.2373(20)	0.2418(11)	0.2429(14)	0.2442(11)	0.2427(9)	0.2431(7)	0.2403(23)
	z	0.3440(14)	0.3447(10)	0.3452(13)	0.3453(10)	0.3458(8)	0.3450(6)	0.3514(24)
	B(Å^2)	1.56(75)	0.08(23)	0.37(30)	0.49(23)	1.37(20)	1.78(18)	1.75(56)
$Fe_1(Ti_1)$	*x*	0.0846(18)	0.0826(8)	0.0844(10)	0.0846(7)	0.0840(6)	0.0851(4)	0.0839(12)
	z	0.6090(12)	0.6057(7)	0.6056(9)	0.6054(6)	0.6050(4)	0.6046(3)	0.6065(11)
	B(Å^2)	1.18(39)	0.53(22)	0.63(26)	0.52(19)	1.46(15)	1.25(11)	1.19(32)
$Fe_2(Ti_2)$	*x*	0.0724(21)	0.0658(8)	0.0654(9)	0.0648(6)	0.0648(5)	0.0634(4)	0.0630(10)
	z	0.1116(13)	0.1117(6)	0.1093(8)	0.1102(5)	0.1103(4)	0.1111(3)	0.1107(11)
	B(Å^2)	0.93(39)	0.06(22)	0.07(25)	-0.01(18)	0.89(13)	0.83(11)	0.22(30)
	x	0.2970(64)	0.2886(28)	0.2849(32)	0.2849(24)	0.2881(16)	0.2922(12)	0.2841(34)

O_1	*z*	0.6687(90)	0.6648(25)	0.6585(31)	0.6567(23)	0.6557(14)	0.6529(11)	0.6522(33)
	B(Å^2)	0.75(36)	1*	1*	1*	1*	1*	1*
O_2	*x*	0.3769(39)	0.3841(26)	0.3819(30)	0.3851(22)	0.3832(15)	0.3848(11)	0.3828(31)
	z	-0.0242(45)	0.9776(26)	0.9751(29)	0.9722(21)	0.9775(15)	0.9807(12)	0.9778(30)
	B(Å^2)	0.75(36)	1*	1*	1*	1*	1*	1*
O_3	*x*	0.4740(63)	0.4775(31)	0.4815(35)	0.4789(25)	0.4776(17)	0.4758(14)	0.4799(38)
	z	0.2142(48)	0.2199(25)	0.2190(29)	0.2207(21)	0.2196(14)	0.2171(12)	0.2158(31)
	B(Å^2)	0.75(36)	1*	1*	1*	1*	1*	1*
O_4	*x*	0.0823(51)	0.0835(28)	0.0840(32)	0.0802(24)	0.0813(16)	0.0781(13)	0.0741(36)
	z	-0.0654(39)	0.9205(22)	0.09240(26)	0.9243(19)	0.9236(13)	0.9252(10)	0.9274(24)
	B(Å^2)	0.75(36)	1*	1*	1*	1*	1*	1*
Statistical parameters								
N-P+C		4270	3108	3120	3076	3152	3138	2891
R_{wp}		0.725	14.2	13.2	13.3	11.8	11.1	9.91
R_{exp}		0.37	10.19	10.11	10.48	8.34	8.91	9.36
χ^2		3.88	1.96	1.71	1.61	2	1.56	1.12
R-Bragg		13.1	8.23	8.2	8.86	6.63	4.48	6.29

* not refined.

Table 2. Evolution of Fe(Ti)-O distances along the $CaFe_2O_4$-$NaFeTiO_4$ solid solution

x	**0**	**0.2**	**0.4**	**0.5**	**0.6**	**0.8**	**1**
Fe_1-O distances (Å)							
Fe_1-O_1	2.032(14)	2.000(27)	1.930(32)	1.923(23)	1.954(2)	1.971(12)	1.901(33)
Fe_1-O_2 (×2) (a)	2.049(9)	2.057(19)	2.071(23)	2.085(17)	2.044(11)	2.013(8)	2.048(24)
Fe_1-O_2 (b)	2.039(13)	2.036(26)	2.055(30)	2.015(22)	2.048(15)	2.055(11)	2.054(31)
Fe_1-O_3 (×2)	1.976(10)	2.014(19)	2.020(22)	2.024(16)	2.012(11)	1.994(8)	1.978(24)
<Fe_1-O> (average)	2.020(10)	2.030(21)	2.028(25)	2.026(18)	2.019(12)	2.007(9)	2.001(27)
σ^2(Fe_1-O) (Å^2)	0.00067	0.00048	0.00236	0.00191	0.00107	0.00067	0.00305
Fe_2-O distances (Å)							
Fe_2-O_1 (×2)	2.038(10)	2.091(19)	2.100(22)	2.093(16)	2.069(11)	2.040(8)	2.087(23)
Fe_2-O_3	2.020(15)	1.981(28)	1.999(32)	1.981(23)	1.995(16)	2.014(12)	2.013(36)
Fe_2-O_4 (×2) (a)	2.098(11)	2.064(18)	2.061(21)	2.034(15)	2.037(10)	2.011(8)	1.985(22)
Fe_2-O_4 (b)	1.963(14)	2.057(25)	1.998(29)	2.002(21)	2.011(14)	2.001(11)	1.970(29)
<Fe_2-O> (average)	2.0425(8)	2.058(21)	2.053(24)	2.039(17)	2.036(12)	2.019(9)	2.021(26)
σ^2(Fe_2-O) (Å^2)	0.00216	0.00136	0.00175	0.00177	0.00075	0.00026	0.00233

Fe-O-Fe angles (°)							
Fe_1-O_1-Fe_2	118.2(7)	121.5(1)	123.6(1)	124.3(9)	124.2(6)	124.7(5)	126.4(1)
Fe_2-O_1-Fe_2	96.3(5)	91.7(8)	90.7(9)	90.8(6)	91.9(4)	93.3(3)	90.4(9)
Fe_1-O_2-Fe_1	91.1(5)	93.7(8)	92.3(9)	91.3(6)	93.4(5)	95.0(4)	92.6(9)
Fe_1-O_2-Fe_1	98.0(6)	99.2(1)	98.6(1)	99.3(9)	99.0(6)	99.9(5)	98.4(1)
Fe_1-O_3-Fe_1	101.1(5)	96.3(8)	95.4(9)	94.8(6)	95.4(4)	96.2(3)	97.0(9)
Fe_1-O_3-Fe_2	129.5(7)	131.8(1)	132.2(1)	132.6(9)	132.3(6)	131.9(5)	131.4(2)
Fe_2-O_4-Fe_2	101.5(6)	96.5(9)	96.6(1)	97.8(8)	97.4(6)	98.6(4)	99.9(1)
Fe_2-O_4-Fe_2	90.5(5)	93.2(7)	92.9(8)	94.2(6)	93.8(4)	95.1(3)	96.5(9)

Table 3. Irreductible representations of the space group Pnma at point K[000].

Representation	$(2_x/½½0)$	$(2_y/0½½)$	$(\bar{1}/000)$	Eigefunctions in the chemical unit cell		
				x	*y*	*z*
Γ_1	1	1	1			C
Γ_2	1	-1	1	F	C	
Γ_3	-1	1	1	C	F	
Γ_4	-1	-1	1			F
Γ_5	1	1	-1	G	A	
Γ_5	1	-1	-1			A
Γ_7	-1	1	-1			G
Γ_8	-1	-1	-1	A	G	

Table 4. Results of Rietveld refinements on $CaFe_2O_4$ XRD and neutron data at low temperature. Space group Pnma.

	X-rays (10 K)			**neutrons (2 K)**		
Cell parameters (Å)						
	a	*b*	*c*	*a*	*b*	*c*
	9.218 (1)	3.0140 (4)	10.697 (2)	9.218 *	3.014 *	10.697 *
Positional parameters						
	x	*y*	*z*	*x*	*y*	*z*
Ca	0.243 (4)	0.25	0.340 (3)	0.191(11)	0.25	0.330(10)
Fe1	0.087 (3)	0.25	0.606 (2)	0.088 (5)	0.25	0.608 (3)
Fe2	0.067 (3)	0.25	0.113 (2)	0.032 (7)	0.25	0.109 (4)
O1	0.319 (8)	0.25	0.662 (8)	0.352 (5)	0.25	0.672 (9)
O2	0.379 (7)	0.25	0.969 (7)	0.410 (7)	0.25	0.963 (8)
O3	0.471 (9)	0.25	0.214 (7)	0.459 (8)	0.25	0.222(11)
O4	0.091 (8)	0.25	0.931 (7)	0.118 (6)	0.25	0.957(11)
Magnetic parameters						
				M(Fe1)	4.50 (39)	

						M(Fe2)	-1.77 (32)	
Statistical parameters								
	N(variables)	R_{wp}	R_{exp}	χ^2	R_{Bragg}	*N(variables)*	R_{wp}	χ^2
	22	43.6	33.8	1.66	7.79	17	5.7	5.8

* not refined.